**Michael A. Marr**

**James S. Wallace**[1]
e-mail: wallace@mie.utoronto.ca

**Larry Pershin**

**Sanjeev Chandra**

**Javad Mostaghimi**

Department of Mechanical and Industrial Engineering,
University of Toronto,
Toronto, ON, M5S 3G8, Canada

# Preliminary Testing of Metal-Based Thermal Barrier Coating in a Spark-Ignition Engine

*A novel metal-based thermal barrier coating was tested in a spark-ignition engine. The coating was applied to the surface of aluminum plugs and exposed to in-cylinder conditions through ports in the cylinder wall. Temperatures were measured directly behind the coating and within the plug 3 and 11 mm from the surface. In-cylinder pressures were measured and analyzed to identify and quantify knock. Test results suggest the coating does not significantly reduce overall heat transfer, but it does reduce the magnitude of temperature fluctuations at the substrate surface. It was found that heat transfer can be reduced by reducing the surface roughness of the coating. The presence of the coating did not promote knock.* [DOI: 10.1115/1.4000298]

## 1 Introduction

Much of the research on thermal barrier coatings (TBCs) in internal combustion engines has focused on "adiabatic" diesel engines. Adiabatic engines utilize thick ceramic coatings to significantly increase combustion chamber surface temperatures and reduce net heat losses. The adiabatic concept is limited to diesel engines because significantly higher wall temperatures would cause pre-ignition and knock in spark-ignition (SI) engines. However, if used sparingly to induce only modest wall temperature increases, TBCs may have beneficial applications for SI engines.

Moderately elevated wall temperatures have been shown to reduce accumulation of knock-promoting carbonaceous deposits [1]. In SI engines, retarding spark timing or switching to higher octane fuel is required over time to prevent knock as deposits build up. Therefore, if peak wall temperatures can be raised enough to reduce deposit buildup but not so much to induce autoignition, a TBC could reduce the need for changing spark timing or fuel. Furthermore, as heat is transferred from the wall to the gas during the intake stroke, a TBC could reduce charge temperatures and increase volumetric efficiency [2]. These performance improvements have been demonstrated experimentally with thin ceramic coatings. Assanis and Mathur [3] tested a SI engine with the combustion chamber coated with a 0.10–0.27 mm thick ceramic, and found the coating improved power and fuel efficiency and increased exhaust gas temperatures without increasing knock occurrence. Mendera [4] found that a thin 0.2–0.4 mm thick ceramic coating on the piston improved fuel consumption.

In two-stroke SI engines, thermal barrier coatings have been shown to improve fuel evaporation and combustion, thereby reducing carbon monoxide (CO) and hydrocarbon (HC) emissions [5,6]. Furthermore, two-stroke engines typically run rich and elevated wall temperatures allow for leaner operation to further improve fuel efficiency and reduce emissions.

Thermal barrier coatings can also protect against thermal fatigue by reducing the magnitude of cyclic temperature fluctuations experienced by coated substrate. Coating application could be targeted to components that are particularly susceptible to thermal fatigue.

One of the primary reasons ceramic TBCs have not been more widely adopted is their lack of durability when exposed to engine conditions [7]. Overtime, ceramic coatings have a tendency to fail and lose adhesion to the metal substrate.

To overcome the durability issues associated with ceramics, research is underway to develop metal-based TBCs. This study focuses on one particular coating made from a nanostructured iron-based refractory powder applied by wire arc technique. The coating demonstrated excellent fracture resistance during imprint hardness testing. Relevant coating properties are summarized in Table 1 [8]. In terms of thermal conductivity, the coating is similar to silicon nitride and only about five times more conductive than partially stabilized zirconia [9]. The combination of low thermal conductivity with good fracture resistance and thermal expansion close to engine metals suggest the TBC is well suited for combustion chamber surfaces such as the piston crown and cylinder head. The coating's hardness and roughness likely rule out its use on rubbing surfaces such as the cylinder wall.

The purpose of this study is to test the metal-based TBC in a SI engine. The coating was applied to the face of aluminum plugs, which were inserted into ports in the cylinder wall for exposure to in-cylinder conditions. Thermocouples were installed in the plugs to measure their internal temperature. For some tests, a fast response thermocouple was used to measure instantaneous substrate temperatures directly behind the coating. Additionally, in-cylinder pressure data were analyzed to determine if the coating increases the occurrence of knock.

## 2 Experimental Setup

All tests were conducted on a single cylinder Cooperative Fuels Research (CFR) engine coupled to a dc dynamometer. 87 octane regular pump gasoline was used and the engine compression ratio was approximately 8.7:1. Unless indicated otherwise, spark timing was set at 20 deg crank angle (degCA) before top center (TC) for maximum brake torque. For all tests, the engine was run wide open throttle at 1500 rpm with a stoichiometric fuel air mixture.

The CFR engine was chosen because it features three threaded access ports around the cylinder perimeter as illustrated in Fig. 1. The access ports provide ready access to the combustion chamber and great flexibility in testing various coated specimens in different combinations. Plugs were machined from an engine casting aluminum alloy cylinder head to be threaded into the ports, and the coatings were applied to the plug faces for exposure to in-

[1]Corresponding author.

Contributed by the IC Engine Division of ASME for publication in the JOURNAL OF ENGINEERING FOR GAS TURBINES AND POWER. Manuscript received May 21, 2009; final manuscript received May 22, 2009; published online April 21, 2010. Editor: Dilip R. Ballal.

**Table 1 Approximate coating properties**

| | |
|---|---|
| Thickness | 0.5 mm |
| Thermal diffusivity | $1.8\times10^{-6}$ $m^2/s$ |
| Density | $6.4\times10^{3}$ $kg/m^3$ |
| Specific heat capacity | 0.43 kJ/kg K |
| Thermal conductivity | 5 W/m K |
| Porosity | 8.9% |
| Coefficient of thermal expansion | $15\times10^{-6}$ $K^{-1}$ |

cylinder conditions. A drawing of the plugs is shown in Fig. 2. Teflon tape was wrapped around the plug threads to minimize heat transfer through them.

To monitor internal plug temperatures, two holes were drilled in each plug to allow for insertion of type K thermocouples to depths of 3 mm and 11 mm from the face. The thermocouples were held in place with a room temperature vulcanizing silicon gasket compound, and a thermally conductive paste was used to minimize contact resistance between the thermocouple junction and the plug to ensure accurate measurement. Throughout this document, thermocouple locations will be referred to by their access port and distance from plug face. For example, the thermocouple in access port B that is 3 mm from the face will be referred to as "B3."

The plug thermocouples and an inlet temperature thermocouple were connected to a National Instruments PCI-6220 data acquisition board through a SCB-68 termination block. The data acquisition board has eight double-ended analog inputs with cold junction compensation for thermocouples. A virtual instrument (VI) program was written using LABVIEW software to acquire six channels of thermocouple data as a function of the elapsed time of the test. Temperature data were acquired at 1000 samples/s, filtered with a 100 Hz low pass filter, and then averaged over 1 s intervals. The type K thermocouple calibration built in to LABVIEW software was used to generate temperature data from the raw thermocouple voltages. The calibration of all thermocouples were checked against a physical ice point and against boiling water, and both checks provided satisfactory agreement.

During engine operation, torque, speed, oil temperature, cooling water temperature, exhaust temperature and exhaust oxygen content were also monitored to maintain consistent test conditions.

Before collecting data, the engine was warmed up for at least 5 min at idle and 7 min at full load. By this time, the cooling water temperature had stabilized at its boiling point and plug temperatures were approximately steady. It was attempted to perform every test under similar conditions, although this was impossible due to changes in ambient conditions, oil temperature, etc. To provide a universal measure of test conditions, an uncoated plug was left in port A throughout all tests (except the knock tests).

Most of the data presented are averages from repeated testing cycles. The error bars are shown in Figs. 3–6 and 11 to indicate the variation between testing cycles. The bars represent the 95% confidence interval for the sample.

More specific testing details will be discussed when relevant in Sec. 3.

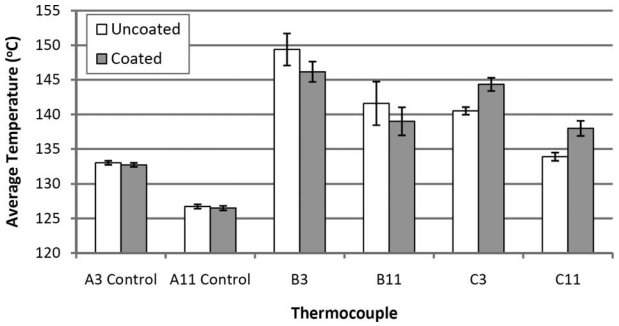


**Fig. 3 Internal plug temperatures**

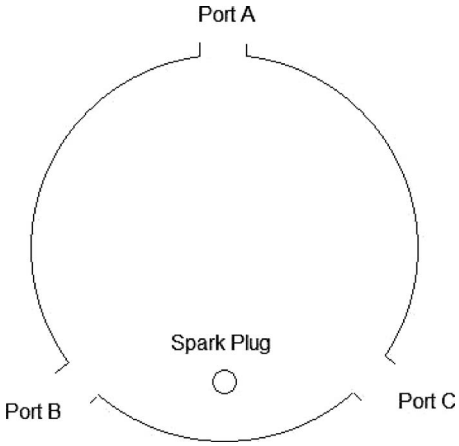


**Fig. 1 Cylinder wall access port configuration**

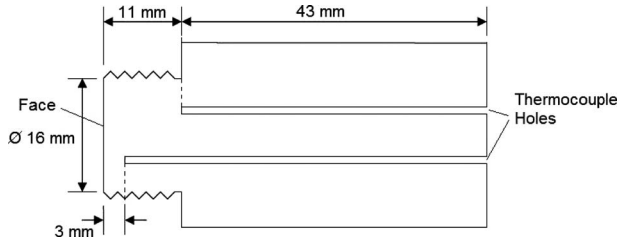


**Fig. 2 Aluminum plug drawing**

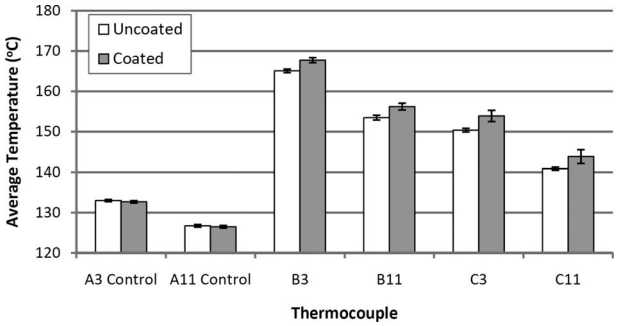


**Fig. 4 Internal plug temperatures with damaged thread plug**

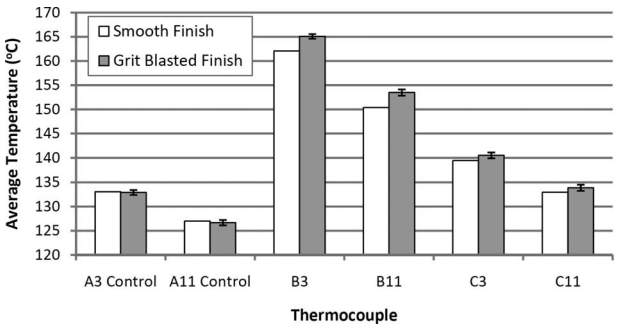


**Fig. 5 Effect of surface finish on uncoated plug**

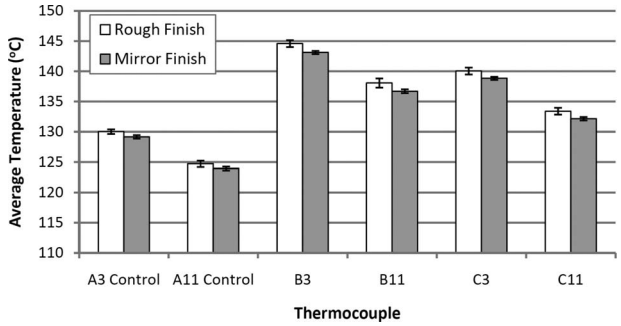


**Fig. 6 Effect of surface finish on coated plug**

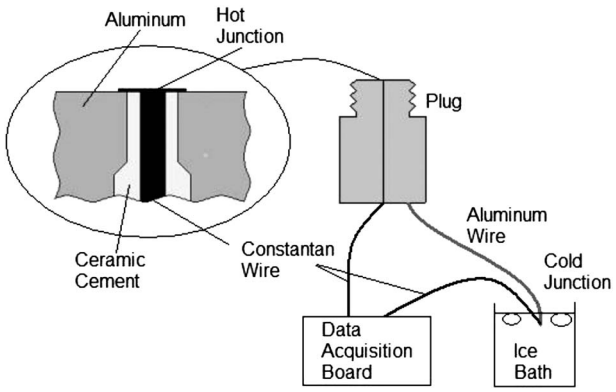


**Fig. 7 Fast response thermocouple schematic**

## 3 Results and Discussion

Experimental coated and uncoated internal plug temperatures are shown in Fig. 3. The same plugs were used for both the coated and uncoated tests. In other words, a set of uncoated plugs was tested, the coating was applied, and then they were tested again.

During fabrication of one the plugs, an error was made in the threading process that produced shallow threads in some spots. When installed in the cylinder wall, this plug would run up to 15°C hotter than the other plugs with good threads. This difference is likely due to increased thread contact resistance reducing heat transfer from the plug to the cooled engine block. Therefore, to investigate the coating's performance on a hotter substrate, the damaged threads plug was also tested and the results are shown in Fig. 4. The damaged threads plug was tested in both ports B and C.

Figures 3 and 4 generally show higher temperatures in the coated plugs, suggesting the coating increased net heat flux to the engine wall. Only thermocouples B3 and B11 in Fig. 3 show reduced temperatures after coating, although these differences are not statistically significant to a 95% confidence level when checked with a student's *t*-test. On the other hand, the thermocouple data that show temperature increases after coating (Fig. 3: C3 and C11, and Fig. 4: B3, B11, C3, and C11) are all statistically significant. This result is unexpected, but there are possible explanations for the temperature increases.

During intake and early compression, heat is transferred from the combustion chamber surfaces to the cooler intake gas. It is possible that the coating reduces heat flow in this direction more than it reduces heat flow in the primary direction from the gas to the wall. This would effectively increase net heat transfer and plug temperatures.

A second explanation is that surface roughness increases convective heat transfer by changing the microscopic area available for heat transfer. This effect is supported by Tsutsumi et al. [10], who found that applying a mirror finish to combustion chamber surfaces reduces component temperatures and overall heat transfer. In the present study, the metal coating had a very rough finish, while the uncoated plug face had a much smoother machined finish.

A point of interest in Figs. 3 and 4 is the temperature difference between ports B and C, which are near the inlet valve and exhaust valve, respectively. This engine was not designed to generate swirl, and therefore the authors do not believe the temperature difference is due to asymmetrical gas motion. Instead, the difference is likely because of uneven cooling, due to differences in proximity to coolant passages and coolant circulation patterns.

**3.1 Effect of Surface Roughness.** Two experiments were performed to investigate the effect of surface roughness on coating performance. The first experiment measured temperatures of uncoated plugs before and after grit blasting was performed to increase roughness. The results are shown in Fig. 5. It should be noted that the smooth finish only experienced one testing cycle before grit blasting, and therefore no error bars are shown on those temperatures. Also, the plug with damaged threads was used in port B, which is the reason for the considerably higher temperatures measured there.

The second experiment on surface roughness measured temperatures in a coated plug before and after polishing to a mirror finish. The results are shown in Fig. 6.

Figures 5 and 6 both show internal plug temperatures were higher with the rougher surface finish, suggesting roughness does have an effect on heat transfer through the coating.

**3.2 Effect of Coating on Substrate Surface Temperature.** To measure temperatures at the substrate surface, a new plug was fabricated with a fast response thermocouple having its hot junction at the surface. The design, which utilized the aluminum plug body as one of the two thermocouple metals, was based upon a previous thermocouple developed by Heichal et al. [11]. A schematic of the thermocouple is shown in Fig. 7. The plug was fabricated out of 6061 aluminum because no more engine cast aluminum was available.

To make the thermocouple, a 1/16 in. (1.6 mm) diameter hole was drilled from the back end of the plug to approximately 10 mm from the face. A 0.5 mm diameter hole was then drilled through the face until it connected with the 1/16 in. hole. Bare 0.25 mm diameter constantan wire was fed through the hole and held in place with Omega CC high temperature cement. After the cement had cured, the plug face was polished with crocus cloth until the wire and cement were flush with the surface. The resistance between the wire and the plug was checked to confirm electrical isolation. The hot junction was formed by a thin smear of silver-based electrically conductive epoxy (Duralco 124) applied to the area around the wire. The epoxy was cured and then polished until resistance was approximately 15 Ω, at which point it could no longer be felt with bare fingertips.

The thermocouple's response time was not measured, but Heichal et al. [11] achieved response times of 10 ns with their thermocouples, which were identical to this study's design except Heichal et al. formed the hot junction with a graphite smear. As a response time on the order of 10 $\mu$s is required for engine measurements, it was assumed that this study's thermocouple was sufficiently fast.

To complete the thermocouple loop, an aluminum wire was clamped to the plug and joined with another constantan wire in an ice bath to form the cold junction. The voltage difference between the two constantan wires was measured by the data acquisition board. The thermocouple was calibrated from room temperature to 250°C to find a third-order polynomial for the temperature-voltage relationship. Over this range, the average output was 44 $\mu$V/°C.

The data acquisition board was switched to a National Instruments PCI-6251 for its high sampling rate capabilities. The crank

**Table 2 Summary of substrate surface temperature results**

| Average temperatures (°C) | Uncoated | Coated |
|---|---|---|
| Substrate surface cycle average | 157.1 | 152.9 |
| Substrate surface cycle minimum | 149.8 | 151.1 |
| Substrate surface cycle maximum | 194.3 | 154.7 |
| A3 control | 132.5 | 131.4 |
| A11 control | 127.2 | 125.8 |

shaft was equipped with a BNC H25 encoder to provide a 0.2 degCA interval sampling time base, making the sampling rate 45 kHz at 1500 rpm. The encoder's once per revolution *Z* pulse was used to determine exact crank shaft position. A 51 point moving average smoothing algorithm was used to minimize signal noise.

The fast response plug was tested uncoated to develop a baseline, then coated and tested again. 600 cycles of temperature data were recorded for both the uncoated and coated conditions. All measurements were taken in port C.

Table 2 summarizes the results of the substrate surface temperature measurements, and Fig. 8 shows two consecutive cycles of uncoated and coated temperatures. The average temperature was lower after the coating was applied. However, this result should be viewed with caution, as the A3 and A11 control temperatures were also lower during the coated tests. Additionally, the thermocouple's presence alters the temperature profile within the substrate, meaning the measured temperatures are not the same as they would be without the thermocouple. This consideration will be discussed in more detail shortly.

Despite the thermocouple considerations, it is clear that the coating significantly damps cyclic temperature fluctuations at the substrate surface. The significance of the damping effect is evident in Fig. 8, where temperature swings are hardly visible when coated. Temperature swings for each individual cycle are presented in Fig. 9, from which it is apparent that the uncoated substrate was seeing large cyclic fluctuations.

*3.2.1 Fast Response Thermocouple Considerations*. The thermocouple's presence alters the regular temperature profile of the substrate because the cement, constantan, and silver epoxy have different thermal properties than aluminum, including lower thermal conductivities. Therefore, the temperatures in Table 2 and Figs. 8 and 9 may not be representative of the "true" surface temperatures that would exist if the substrate was entirely aluminum. To gain insight into the difference between measured and true substrate surface temperatures, finite element method (FEM) was used to model the thermocouple under heat flux conditions typical of a SI engine. The FEM analysis is explained and discussed in detail in the Appendix.

The results of the FEM analysis suggest the thermocouple overestimates both cycle averaged temperatures and the magnitude of temperature swings. However, the thermocouple is considerably

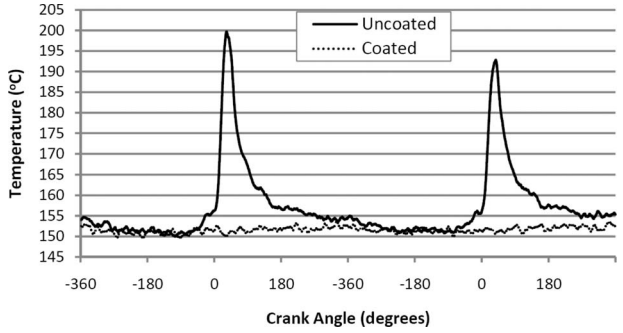


**Fig. 8 Sample substrate surface temperatures**

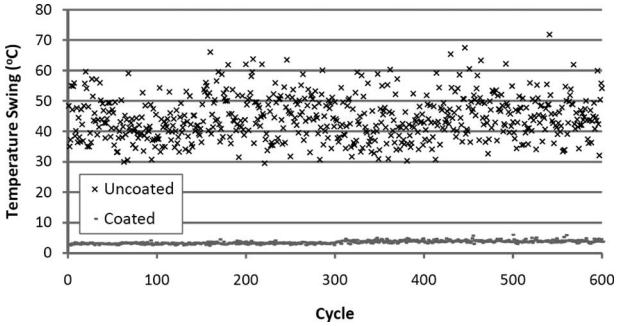


**Fig. 9 Individual cycle peak-to-peak temperature swings at substrate surface**

more accurate when under the coating. Regarding average temperatures, it was found that the uncoated difference between measured and true values is approximately twice as large as the coated difference. For example, at high heat flux, the uncoated thermocouple overestimates average temperatures by 10.4°C, while the coated thermocouple overestimates by only 5.2°C. Regarding temperature swings, it was found that the thermocouple overestimated temperature swings by 170–230% when uncoated, but only by 120% when coated.

The FEM analysis shows that extreme caution should be used when interpreting the surface thermocouple measurements. The surface temperature measurements are most useful to demonstrate that the coating does significantly damp temperature fluctuations. In future studies, the thermocouple should be made as small as possible and have thermal properties that closely match the substrate.

**3.3 Discussion of Coating Performance as Thermal Barrier.** The temperature measurements obtained in this study do not definitively show that the coating increased or decreased net heat transfer. Temperatures measured within the substrate generally suggest the coating increased net heat transfer, but this result was not unanimous. Either way, the temperature difference between the uncoated and coated conditions was small, never being more than 3–4°C.

There are two main reasons why the coating may not be very effective at reducing net heat transfer despite its low thermal conductivity. First of all, the coating may be reducing heat transfer from the wall to the gas during the portion of the cycle when heat flows in this direction. This would prevent the substrate from cooling down as much as it would if it were uncoated. Table 2 shows that minimum instantaneous temperatures were lower at the substrate surface when it was not coated. Second, the coating's rough surface finish may be increasing convective heat transfer. This reason is supported by Figs. 5 and 6, which show higher plug temperatures with rougher surface finishes.

While the coating may not significantly reduce net heat transfer, it significantly damps out temperature fluctuations at the substrate surface. This performance characteristic supports its use as a protective coating for components that are susceptible to thermal fatigue.

The effect of the coating on deposit accumulation was not investigated in depth in this study. If the coated surface has higher peak temperatures than an uncoated surface, it could reduce deposit accumulation. Future studies should include a more detailed consideration of deposits.

It should be mentioned that it is difficult to avoid variation between coatings, and each coated plug tested in this study certainly had different thermal properties. The values listed in Table 1 are approximate average values determined from multiple samples. Variation in adhesion, porosity, composition, and other characteristics may be responsible for some of the discrepancies present in the results.

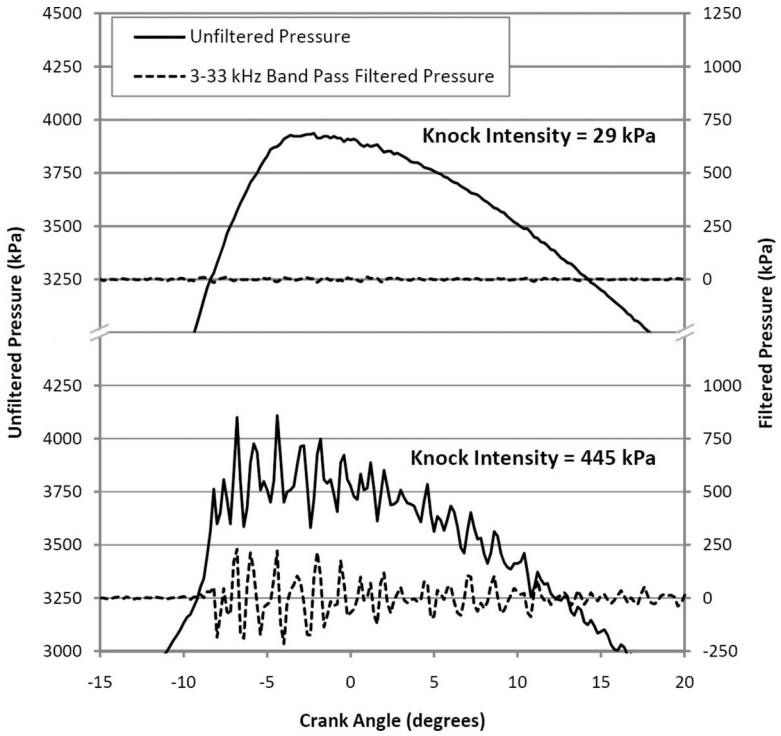


**Fig. 10 Sample cycles with different knock intensities**

**3.4 Effect of Coating on Knock.** Tests were conducted to determine if the coatings increased the incidence of knock. Knock was identified and quantified through analysis of in-cylinder pressure data. To measure in-cylinder pressure, a Kistler 6125B piezoelectric pressure transducer was installed in port B in a slotted adapter designed according to previous work by Randolph [12]. The transducer was connected by high impedance cable to a Kistler Type 5010 charge amplifier and then to a National Instruments PCI-6071E high speed data acquisition board through a BNC-2080 termination block. A Kistler Type 5311A 33 kHz low pass filter was used to remove signal noise due to the transducer's natural frequency and resonance in the slotted adapter. As with the substrate surface temperature tests, the encoder provided the timing signal in 0.2 degCA intervals.

Knock intensity was defined as the peak-to-peak amplitude of the 3–33 kHz band pass filtered pressure signal. Alternative knock indicators have been used; the authors chose this method for its simplicity. The 3–33 kHz range was chosen to capture the first three circumferential modes of acoustic vibration, which are the most dominant pressure wave frequencies during knock [13]. In the CFR engine, these modes should occur between 6 kHz and 15 kHz [14]. The 3 kHz high pass filter was a software third-order Butterworth type filter, and the low pass filter was the Type 5311A filter described above. Figure 10 provides two examples of filtered and unfiltered pressure signals for cycles with different levels of knock.

New plugs were used for these tests to minimize the influence of deposits. The plugs were installed in ports A and C. A 1000 W heater was installed in the inlet air line to help promote knock. The heater was regulated with an Omega CN9000A temperature controller to maintain intake temperatures of 35°C and 65°C. As with all other tests in this study, the engine was run at 1500 rpm, and wide open throttle and sufficient warm up time was provided before measurements were taken. Spark timing was adjusted to 40 degCA advanced of TC to further promote knock.

The results of the knock tests are in Fig. 11. Each bar represents the average of approximately 600 cycles, and knock intensities values for individual cycles were between 20 kPa and 1250 kPa. The results show that average knock intensity levels were slightly lower with the coated plugs installed. However, this result should not be interpreted as a reduction in knock because the coated area was only a small fraction of the total combustion chamber surface area. Rather, it should be concluded that the coating did not promote knock during these tests. Tests with a larger coated surface area are required to more rigorously investigate the coating's effect on knock levels. These tests could show an increase in knock due to higher surface temperatures or a decrease in knock if deposit accumulation is reduced.

It should be noted that the knock levels measured were relatively low. In future tests, it would be advantageous to increase the compression ratio or use a lower octane fuel to increase knock intensity.

## 4 Conclusions and Recommendations

In this preliminary study, a metal-based TBC was tested in a spark-ignition engine. The coating was applied to the face of aluminum plugs which were installed in ports around the cylinder wall. Temperatures were measured directly behind the coating and deeper within the plug, and in-cylinder pressure data were analyzed to identify and quantify knock. Based on the results, the following conclusions are drawn.

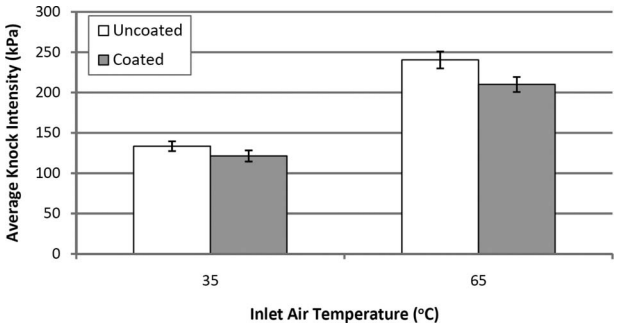


**Fig. 11 Average knock intensity**

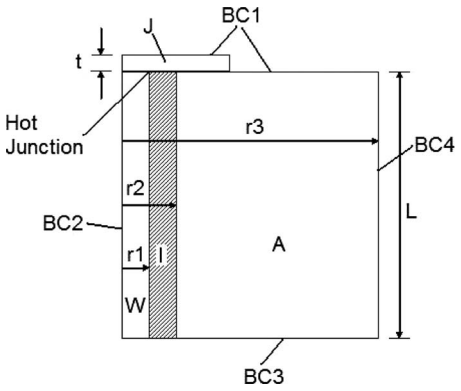


**Fig. 12 Uncoated geometry**

1. The coating did not significantly reduce net heat transfer to the plugs. In some tests the coating reduced plug temperatures, and in other tests it increased plug temperatures. In both cases, the difference between the uncoated and coated temperatures was always small, never being more than 3–4 °C.
2. The coating significantly reduced temperature fluctuations at the substrate surface. It may therefore have applications as a protective coating for components that are susceptible to thermal fatigue.
3. Reducing surface roughness reduced heat transfer through the coating, as demonstrated by a reduction of plug temperatures after the coating was polished to a mirror finish. A similar effect was observed with uncoated plugs that increased in temperature after being grit blasted.
4. The presence of the coating did not increase knock.

Much more research is required to investigate and verify the conclusions of this study. The authors are currently developing an experiment to test the coating on a piston crown, which will provide a larger and hotter surface for testing. The experiment will also investigate the coating's ability to reduce deposit accumulation. The piston will be instrumented to measure instantaneous temperature and heat flux at multiple locations. Improvements will be made to the fast response thermocouples to increase their accuracy.

## Acknowledgment

The authors would like to thank the BMW Technology Office in Palo Alto and the Natural Sciences and Engineering Research Council of Canada (NSERC) for their financial support of this study. The authors are also grateful for the guidance and assistance of Azita Khalili and Jan Tribulowski of BMW, François Gitzhofer of the Université de Sherbrooke, Jean-Gabriel Legoux of NRC Industrial Materials Institute, and Tom Coyle of the University of Toronto.

## Appendix: Finite Element Analysis of Fast Response Thermocouples

COMSOL multiphysics FEM software was used to model the fast response thermocouples under transient heat flux conditions typical of a cylinder wall. The thermocouple was modeled for both the uncoated and coated cases. The uncoated geometry is shown in Fig. 12, and the coated geometry was identical except it had a 0.5 mm thick coating layer and no junction. The parameters used are listed in Table 3. The model was two-dimensional axial symmetric in cylindrical coordinates to provide a three-dimensional equivalent output.

Figure 13 shows the transient convective heat transfer coefficient and gas temperature that were used to calculate heat transfer into the top surface. The convective heat transfer coefficient was calculated by the Woschni equation [15], and gas temperature and pressure data were taken from previous SI engine work by Enomoto and Furuhama [16]. Figure 13 provides a reasonable estimate of heat transfer conditions in a SI engine at 1500 rpm, but it is not necessarily representative of the heat transfer conditions present during this study's experiments.

**Table 3 Model parameters**

| Dimensions | | |
|---|---|---|
| $L$ | 8 mm | |
| $r1$ | 125 $\mu$m | |
| $r2$ | 250 $\mu$m | |
| $r3$ | 5 mm | |
| $t$ (uncoated model) | 2 $\mu$m | |
| Coating thickness (coated model) | 500 $\mu$m | |
| **Material properties** | **$k$(W/m K)** | **$\alpha$ (m$^2$/s)** |
| $A$-aluminum | 142 | $5.6\times10^{-5}$ |
| $I$-cement | 1.2 | $5.1\times10^{-7}$ |
| $W$-constantan wire | 23.5 | $6.4\times10^{-6}$ |
| $J$-silver epoxy (uncoated model) | 7.2 | $2.9\times10^{-6}$ |
| Coating (coated model) | 5.0 | $1.8\times10^{-6}$ |
| **Boundary conditions** | | |
| BC1 | Convection using Fig. 13 | |
| BC2 | Axial symmetry | |
| BC3 | $T$=373.15 K | |
| BC4 | Thermal insulation | |

The geometry was meshed by COMSOL with variable spacing with highest density around the thermocouple. The time step was set at 0.1 ms. Trials found that refining the mesh further or reducing the time step did not substantially alter the FEM output.

Figure 14 shows the FEM output for both the uncoated and coated cases. To obtain temperatures more comparable to the ex-

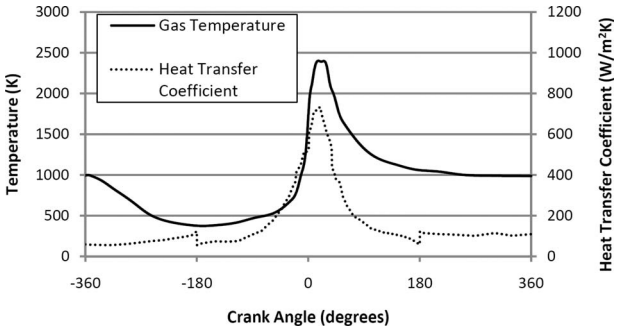


**Fig. 13 Convection data**

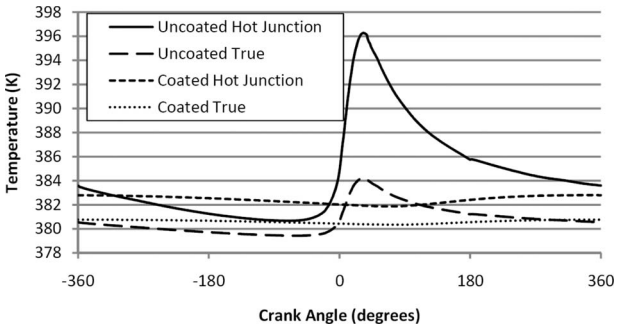


**Fig. 14 FEM output**

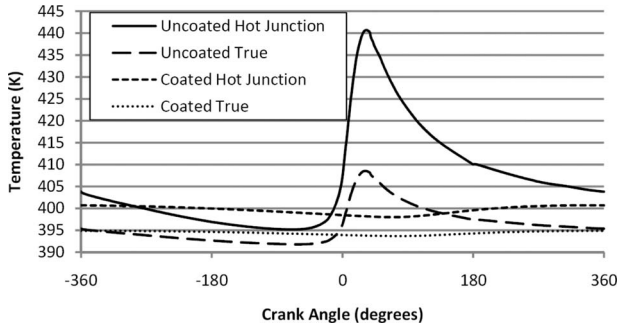


**Fig. 15 FEM output with 3X heat transfer coefficient**

perimental measurements in Table 2 and Figs. 8 and 9, the analysis was also performed with the heat transfer coefficient multiplied by 3, with the output shown in Fig. 15. Table 4 summarizes Figs. 14 and 15.

The output from the FEM analysis indicates that the thermocouple overestimates both the average temperature and the magnitude of temperature swing. With the larger heat transfer coefficient, the average temperature of the uncoated hot junction is 10°C greater than the true average, and the magnitude of uncoated hot junction temperature swing is 29°C greater than the true swing, which corresponds to a 170% overestimate. When coated, the average hot junction temperature is 5°C larger than the true average, and the hot junction temperature swing is only 1.5°C greater but this still corresponds to a 120% overestimate. With the lower heat transfer coefficient, the average hot junction temperatures were closer to true values, but the temperature swing overestimate percentages were similarly high.

**Table 4 FEM results summary**

| | | | Temperatures (K) | |
|---|---|---|---|---|
| Heat Flux | | | Average | Swing |
| Woschni | Uncoated | Hot junction | 384.5 | 15.6 |
| | | True | 380.7 | 4.8 |
| | Coated | Hot junction | 382.4 | 0.9 |
| | | True | 380.6 | 0.4 |
| 3x Woschni | Uncoated | Hot junction | 406.4 | 45.5 |
| | | True | 396.0 | 16.7 |
| | Coated | Hot junction | 399.6 | 2.7 |
| | | True | 394.4 | 1.2 |

## References


[1] Nakic, D., Assanis, D., and White, R., 1994, "Effect of Elevated Piston Temperature on Combustion Chamber Deposit Growth," SAE Technical Paper Series No. 940948.

[2] Kamo, R., Assanis, D., and Bryzik, W., 1989, "Thin Thermal Barrier Coatings for Engines," SAE Technical Paper Series No. 890143.

[3] Assanis, D. and Mathur, T., 1990, "The Effect of Thin Ceramic Coatings on Spark-Ignition Engine Performance," SAE Technical Paper Series No. 900903.

[4] Mendera, K., 2000, "Effectiveness of Plasma Sprayed Coating for Engine Combustion Chamber," SAE Technical Paper Series No. 2000-01-2982.

[5] Moughal, K. and Samuel, S., 2007, "Exhaust Emission Level Reduction in Two-Stroke Engine Using In-Cylinder Combustion Control," SAE Technical Paper Series No. 2007-01-1085.

[6] Poola, R., Nagalingam, B., and Gopalakrishnan, K., 1994, "Performance of Thin-Ceramic-Coated Combustion Chamber With Gasoline and Methanol as Fuels in a Two-Stroke SI Engine," SAE Technical Paper Series No. 941911.

[7] Saad, D., Saad, P., Kamo, L., Mekari, M., Bryzik, W., Schwarz, E., and Tasdemer, J., 2007, "Thermal Barrier Coatings for High Output Turbocharged Diesel Engine," SAE Technical Paper Series No. 2007-01-1442.

[8] Gitzhofer, F., Mostaghimi, J., Pershin, L., Coyle, T., Chandra, S., Wallace, J., and Legoux, J., 2008, "Metal-Based Thermal Barrier Coatings for Internal Combustion Engine: Pilot Research (Confidential Draft Report)," Universite de Sherbrooke, University of Toronto, and Surface Technologies IMI-NRC, unpublished.

[9] Heywood, J., 1988, *Internal Combustion Engine Fundamentals*, McGraw-Hill, New York.

[10] Tsutsumi, Y., Nomura, K., and Nakamura, N., 1990, "Effect of Mirror-Finished Combustion Chamber on Heat Loss," SAE Technical Paper Series No. 902141.

[11] Heichal, Y., Chandra, S., and Bordatchev, E., 2005, "A Fast-Response Thin Film Thermocouple To Measure Rapid Surface Temperature Changes," Exp. Therm. Fluid Sci., **30**(2), pp. 153–159.

[12] Randolph, A., 1990, "Cylinder-Pressure-Transducer Mounting Techniques to Maximize Accuracy," SAE Technical Paper Series No. 900171.

[13] Brunt, M., Pond, C., and Biundo, J., 1998, "Gasoline Engine Knock Analysis Using Cylinder Pressure Data," SAE Technical Paper Series, 980896.

[14] Draper, C., 1938, "Pressure Waves Accompanying Detonation in the Internal Combustion Engine," J. Aeronaut. Sci., **5**(6), pp. 219–226.

[15] Woschni, G., 1967, "A Universally Applicable Equation for the Instantaneous Heat Transfer Coefficient in the Internal Combustion Engine," SAE Trans., **76**, p. 670931.

[16] Enomoto, Y. and Furuhama, S., 1984, "Measurement of the Instantaneous Surface Temperature and Heat Loss of Gasoline Engine Combustion Chamber," Proc. SAE, **1**, pp. 1.58–1.63.